

# Theory of quasi-one dimensional imbalanced Fermi gases

Erhai Zhao and W. Vincent Liu

*Department of Physics and Astronomy, University of Pittsburgh, Pittsburgh, Pennsylvania 15260, USA*

We present a theory for a lattice array of weakly coupled one-dimensional ultracold attractive Fermi gases (1D ‘tubes’) with spin imbalance, where strong intratube quantum fluctuations invalidate mean field theory. We first construct an effective field theory, which treats spin-charge mixing exactly, based on the Bethe ansatz solution of the 1D single tube problem. We show that the 1D Fulde-Ferrel-Larkin-Ovchinnikov (FFLO) state is a two-component Luttinger liquid, and its elementary excitations are fractional states carrying both charge and spin. We analyze the instability of the 1D FFLO state against inter-tube tunneling by renormalization group analysis, and find that it flows into either a polarized Fermi liquid or a FFLO superfluid, depending on the magnitude of interaction strength and spin imbalance. We obtain the phase diagram of the quasi-1D system and further determine the scaling of the superfluid transition temperature with intertube coupling.

## I. INTRODUCTION

The last few years witnessed an explosion of studies in population imbalanced (‘polarized’) Fermi gases, partly fueled by the MIT and Rice experiments with resonantly interacting ultracold  ${}^6\text{Li}$  atoms [1, 2]. One of the motivations of these and following experiments [3, 4, 5, 6] is to search for the Fulde-Ferrel-Larkin-Ovchinnikov (FFLO) state, a spatially modulated superfluid [7]. So far, no evidence of FFLO was found in three dimensional (3D) traps. This is in agreement with the mean field theory prediction that FFLO state only occurs in a tiny region in the phase diagram of 3D polarized Fermi gas [8].

Contrary to 3D, in one dimension (1D), Bethe ansatz [9, 10, 11] and Density Matrix Renormalization Group (DMRG) studies [12, 13] show that a FFLO-like phase (which only has algebraic order) occupies a rather large region in the phase diagram of polarized attractive Fermi gas. Taking these results together, recently Parish *et al* [14] proposed that the most promising regime to realize FFLO state is in quasi-one dimension, i.e., a 2D lattice array of cold atomic ‘tubes’ [15] where the transverse tunneling  $t_\perp$  is weak. They obtained the phase diagram of the quasi-1D system using mean field theory [14]. These works prompted the experimental search for the FFLO phase in quasi-1D atomic gas systems. These highly tunable systems are also ideal for investigating the 1D-to-3D dimensional crossover of superfluids [16].

A few key questions remain open regarding the quantum phases of quasi-1D atomic systems. 1) What is the phase diagram in the limit of small  $t_\perp$ ? In this regime, intratube quantum fluctuations is dominantly strong [16] so the mean field approach of [14] ceases to apply. To find the solution, one has to first answer a related question: 2) What is the low energy effective description for the 1D FFLO phase? An effective theory can yield analytical expressions for the zero and finite temperature correlation functions and serve as a starting point to analyze the instability of 1D FFLO against  $t_\perp$ . Note that a field theory for 1D FFLO state was previously proposed by Yang to describe 1D superconductors in magnetic field [17]. In Yang’s model, spin and charge degrees of free-

dom are assumed decoupled. However, we shall show that this model does not apply to attractive Fermi gases with *finite* spin imbalance (‘magnetization’) because the assumption of spin-charge separation breaks down [13].

In this paper, we answer these open questions using a combination of several well established theoretical techniques. We first develop an effective field theory for the 1D FFLO state, which properly treats the spin-charge mixing in trapped two component atomic gases and fully takes into account the intratube quantum fluctuations. Then we treat the transverse tunneling perturbatively [16] to obtain the phase diagram of a 2D lattice array of weakly coupled 1D Fermi gases, which is an anisotropic 3D system. We also derive the scaling formula for the transition temperature of the quasi-1D FFLO state.

Our approach, based on exact solutions, is complementary to the mean field method of Ref [14], which applies to the opposite limit of large  $t_\perp$ . Taken together, they can provide a more complete understanding of the dimensional crossover of quasi-1D attractive Fermi gases with finite population imbalance, and provide guidance for the experimental search of the quasi-1D FFLO phase.

## II. MODEL

We consider a gas of two-component fermionic atoms, e.g.,  ${}^6\text{Li}$  atoms in hyperfine states  $|F = 1/2, m_f = \pm 1/2\rangle$  (labeled with spin up and down respectively), confined in a highly elongated one dimensional (1D) trap interacting via an attractive contact potential,

$$H_{GY} = -\frac{\hbar^2}{2m} \sum_{i=1}^N \frac{\partial^2}{\partial x_i^2} + g \sum_{i=1}^{N_\uparrow} \sum_{j=1}^{N_\downarrow} \delta(x_i - x_j). \quad (1)$$

This Hamiltonian is known as the Gaudin-Yang model [18, 19]. Here  $m$  is the fermion mass, and the attractive interaction strength  $g \equiv -2\hbar^2/ma_{1D} < 0$ ,  $a_{1D}$  is the effective 1D scattering length and related to the 3D  $s$ -wave scattering length  $a_s$  by [20, 21]

$$a_{1D} = (1.03 - \frac{a_\perp}{a_s})a_\perp,$$

where  $a_{\perp} = \sqrt{\hbar/m\omega_{\perp}}$  is the oscillator length of the transverse confinement of frequency  $\omega_{\perp} \gg \omega_x$ . Let  $N_{\uparrow}$  and  $N_{\downarrow}$  be the number of spin up and down particles respectively, and  $N = N_{\uparrow} + N_{\downarrow}$  the total particle number. We define the linear particle density  $n_L = N/L$ , the population imbalance  $p = (N_{\uparrow} - N_{\downarrow})/N$ , and the dimensionless interaction parameter  $\gamma = 2/(n_L a_{1D})$ . These are experimentally controllable parameters. Some of these numbers are listed in Ref. 22. In the above model Hamiltonian, we have neglected the slowly varying Gaussian trap potential in  $x$  direction,  $V(x) = m\omega_x^2 x^2/2$ , and assumed periodic boundary condition for the system of length  $L$ , as we are interested in the collective behaviors of the population imbalanced gas in the thermodynamic limit. The effect of the trap can be subsequently taken into account using local density approximation.

For technical convenience, we also consider a closely related lattice model, the 1D attractive Hubbard model,

$$H_U = -t \sum_{i,\sigma} (c_{i,\sigma}^{\dagger} c_{i+1,\sigma} + h.c.) - U \sum_i n_{i,\uparrow} n_{i,\downarrow}, \quad (2)$$

with linear particle density  $n_L = n/a$  and population imbalance  $p$ . Here,  $n = n_{\uparrow} + n_{\downarrow}$  is the particle number per site (band filling), and  $a$  is the lattice spacing. We define the Fermi wave vector  $k_{f\sigma} \equiv \pi n_{\sigma}/a$  for each spin species  $\sigma = \uparrow, \downarrow$ , and the FFLO wave vector  $q_{\star} \equiv k_{f\uparrow} - k_{f\downarrow}$ . The Hubbard model can be viewed as the (regularized) lattice version of the continuum Gaudin-Yang model, with  $a$  playing the role of the short distance cutoff. Explicitly, the Gaudin-Yang model corresponds to  $H_U$  in the continuum limit,  $a \rightarrow 0$ , for fixed particle numbers and system length  $L$ , i.e.,  $n \ll 1$ . In this limit, the parameters of  $H_{GY}$  are related to those of  $H_U$  by [23]

$$m = \frac{\hbar^2}{2ta^2}, \quad g = -Ua, \quad \gamma = \frac{U}{2tn}. \quad (3)$$

Finally, the experimental setup [24] searching for quasi-1D FFLO state consists of a 2D square lattice array of 1D tubes, each described by  $H_{GY}$  and coupled to its nearest neighbors by transverse tunneling of amplitude  $t_{\perp}$ ,

$$H_{\perp} = -t_{\perp} \int dx \sum_{\langle i,j \rangle, \nu, \sigma} [\psi_{i,\nu,\sigma}^{\dagger}(x) \psi_{j,\nu,\sigma}(x) + h.c.]. \quad (4)$$

Here  $\psi_{\nu=R/L,\sigma}$  is the fermion field operator for right/left movers with spin  $\sigma = \uparrow, \downarrow$  [25], and  $\langle i, j \rangle$  labels nearest neighbor tubes. Also relevant to our discussion is the intertube Josephson coupling of the form

$$H_J = -J \int dx \sum_{\langle i,j \rangle} [\Delta_i^{\dagger}(x) \Delta_j(x) + h.c.]. \quad (5)$$

The pair operator is defined as  $\Delta(x) = \psi_{R,\uparrow}(x) \psi_{L,\downarrow}(x)$ , and the pair tunneling,  $J \propto t_{\perp}^2$ , is generated by second order hopping process. Intertube coupling establishes transverse coherence between tubes and drives the system through a 1D-to-3D dimensional crossover [16].

### III. SPIN-CHARGE MIXING IN AN IMBALANCED FERMION GAS

We first obtain a low energy effective theory for the Gaudin-Yang model using standard Abelian bosonization [25, 26], which is valid for weak interaction (small  $\gamma$ ). We linearize the spectrum of each spin species around its Fermi points  $\pm k_{f\sigma}$ . Note that the two Fermi momenta differ by  $\delta k_f = k_{f\uparrow} - k_{f\downarrow}$ , since  $N_{\uparrow} \neq N_{\downarrow}$ . We also define the average and difference of Fermi velocities,  $\bar{v}_f = (v_{f\uparrow} + v_{f\downarrow})/2$  and  $\delta v_f = v_{f\uparrow} - v_{f\downarrow}$ . We follow the notation convention of Ref. [25], where the bosonization identity takes the form

$$\begin{aligned} \psi_{R,\sigma}(x) &= \frac{U_{R,\sigma}}{\sqrt{2\pi\alpha}} e^{ik_{f,\sigma}x} e^{-i[\phi_{\sigma} - \theta_{\sigma}]}, \\ \psi_{L,\sigma}(x) &= \frac{U_{L,\sigma}}{\sqrt{2\pi\alpha}} e^{-ik_{f,\sigma}x} e^{i[\phi_{\sigma} + \theta_{\sigma}]} \end{aligned} \quad (6)$$

Here  $\theta_{\sigma}$  is the dual field of boson field  $\phi_{\sigma}$ ,  $U_{R/L,\sigma}$  are the Klein factors, and  $\alpha$  is the short distance cutoff. The bosonized Gaudin-Yang model (1) becomes,

$$\begin{aligned} H_B &= \int \frac{dx}{2\pi} \left[ \bar{v}_f (\nabla \theta_c)^2 + \bar{v}_f^{\pm} (\nabla \phi_c)^2 + \delta v_f \delta k_f \frac{\nabla \phi_c}{\sqrt{2}} \right. \\ &\quad + \bar{v}_f (\nabla \tilde{\theta}_s)^2 + \bar{v}_f^{\pm} (\nabla \tilde{\phi}_s)^2 + \sqrt{2} \bar{v}_f^{\pm} \delta k_f \nabla \tilde{\phi}_s \\ &\quad \left. + \delta v_f (\nabla \theta_c \nabla \tilde{\theta}_s + \nabla \phi_c \nabla \tilde{\phi}_s) + \frac{g}{\pi \alpha^2} \cos(\sqrt{8} \tilde{\phi}_s) \right]. \quad (7) \end{aligned}$$

Here the charge and spin field  $\phi_{c/s} = (\phi_{\uparrow} \pm \phi_{\downarrow})/\sqrt{2}$  are defined in the standard way. We have introduced shifted spin fields

$$\tilde{\phi}_s = \phi_s - \delta k_f x / \sqrt{2}, \quad \tilde{\theta}_s = \theta_s,$$

and a short hand notation  $\bar{v}_f^{\pm} = \bar{v}_f \pm g/\pi$ .

For the unpolarized case,  $p = 0$ , both  $\delta k$  and  $\delta v_f$  vanish, so  $H_B$  is reduced to the sine-Gordon model. With a negative coefficient ( $g < 0$ ), the cosine term is relevant. It is well known that the system, an attractive Fermi gas, is a Luther-Emery liquid where spin and charge separation holds: the charge sector is gapless and described by a Gaussian Hamiltonian and the spin sector is gapped. The algebraic decay of the  $s$ -wave pairing susceptibility, which is most diverging, is determined by the Luttinger parameter in the charge sector.

Finite population imbalance brings several significant differences. First, it introduces a linear ‘‘source’’ term for the (shifted) spin field which acts as an *effective* magnetic field,

$$h = \sqrt{2} \bar{v}_f^{\pm} \delta k_f.$$

But more importantly, it leads to coupling between the spin and charge sector, described by the density and current interaction terms ( $\nabla \theta_c \nabla \tilde{\theta}_s$  and  $\nabla \phi_c \nabla \tilde{\phi}_s$ ) of order  $\delta v_f$  in  $H_B$ . Therefore, Eq. (7) clearly shows that a 1D attractive Fermi gas with finite  $p$  is in general not a spin-charge separated Luther-Emery liquid.

In the limit of very small  $p$ , both  $\delta v_f$  and  $\delta k_f$  are small so we can neglect high order terms  $\propto \delta v_f \delta k_f$  in Eq. (7). Furthermore, in situations where we are allowed to neglect the spin-charge mixing terms  $\propto \delta v_f$  but keep the linear  $\nabla \tilde{\phi}_s$  term  $\propto \delta k_f$ , then Eq. (7) reduces to the spin-charge separated model proposed by Yang to describe quasi-1D superconductors in magnetic field [17],

$$H_Y = \int \frac{dx}{2\pi} \left[ \bar{v}_f (\nabla \theta_c)^2 + \bar{v}_f^+ (\nabla \phi_c)^2 + \bar{v}_f (\nabla \tilde{\theta}_s)^2 + \bar{v}_f^- (\nabla \tilde{\phi}_s)^2 + h \nabla \tilde{\phi}_s + \frac{g}{\pi \alpha^2} \cos(\sqrt{8} \tilde{\phi}_s) \right].$$

Its charge sector is a massless Gaussian, while its spin sector (the second line) is a sine-Gordon Hamiltonian in an *effective* magnetic field  $h$ , which we call  $H_{sGh}$ .  $H_{sGh}$  has been investigated thoroughly by many authors since the pioneer works of Ref. 27, 28. Increasing  $h$  over a critical value  $h_c$  will trigger a phase transition from a Luther-Emery liquid (BCS-like superfluid with algebraic order and spin gap) to a FFLO-like phase in which the spin excitation is also massless and the pair correlation function oscillates at wave vector  $q_*$  on top of the algebraic decay. The spin sector of the 1D FFLO phase of  $H_Y$  can be described as a Luttinger liquid of spin solitons [27]. These solitons are the 1D counterpart of the static order parameter domain walls (more precisely, the Andreev bound states at the domain walls populated by the majority spins [14]) which form a crystal in high dimensional FFLO phases [29].

Based the spin-charge separated Hamiltonian  $H_Y$ , Yang also pointed out that the magnetic field driven BCS-FFLO transition is in the universality class of 2-dimensional classical commensurate-incommensurate transitions [17]. To see this clearly, we can solve  $H_{sGh}$  analytically along the Luther-Emery line to map it onto a free (massive) fermion Hamiltonian by refermionization [25, 26]: the magnetic field  $h$  then plays the role of chemical potential, while  $g$  controls the size of the band gap. As  $h$  is increased to  $h_c$ , the Zeeman energy exceeds the band gap, so the upper band becomes populated by spinless fermions (spin solitons). This general picture holds even away from the Luther-Emery line, where spin solitons become interacting with each other. Thus, Yang's model  $H_Y$  gives an appealing physical picture for the 1D FFLO like phase in terms of soliton liquids, provided that the basic assumption of spin-charge separation holds.

Yet, the spin-charge mixing terms in  $H_B$  have scaling dimensions of 2 and are marginal operators in the renormalization group sense. So they cannot be simply neglected even if their values are small. Moreover, in cold atom experiments the population imbalance  $0 \leq p \leq 1$  can be arbitrary and usually not small. This is drastically different from typical situations in solids where the Zeeman energy is much smaller than the Fermi energy. In general, the spin-charge mixing terms have to be treated on the same footing as other terms in  $H_B$ .

While a direct perturbative analysis of  $H_B$  is possible, it is unclear how well the bosonized Hamiltonian  $H_B$  de-

scribes the system for the case of strong interaction and large population imbalance. For these reasons, we shall adopt an alternative but much more powerful method, which is valid for arbitrary  $(n, p, g)$  and treats the spin-charge mixing effect exactly, to construct the bosonized effective field theory of  $H_{GY}$ . The method is based on the Bethe ansatz solution of the microscopic model  $H_{GY}$  (or  $H_U$ ) and general principles of conformal field theory.

#### IV. EFFECTIVE THEORY FOR THE 1D FFLO PHASE

In this section, we show that despite the spin-charge mixing, the 1D FFLO phase features a more general decoupling of two critical degrees of freedom. In the language of conformal field theory, the 1D FFLO state is a critical phase with two gapless normal modes and it is formally described by the direct product of two Virasoro algebras with central charge  $c = 1$  [30]. Such a “two fluid” description is in accordance to our physical intuition in higher dimensions, e.g., the 3D attractive Fermi gas with population imbalance in the strong interaction (BEC) limit can be described by a fermion-boson mixture with some residue interactions. However, the distinction between bosons and fermions is lost in 1D. Our task is to identify the two normal modes (elementary excitations) and establish their relation with the usual spin/charge excitations.

##### A. Summary of main results

We first present the final results, so readers not interested in technical details may skip the derivation and proceed directly to the next section. The 1D FFLO state is a two component Luttinger liquid described in bosonized form by the effective Hamiltonian

$$H_{\text{FFLO}} = \sum_{i=1,2} \int \frac{dx}{2\pi} u_i [(\nabla \vartheta_i)^2 + (\nabla \varphi_i)^2]. \quad (8)$$

The two normal modes ( $i = 1, 2$ ) are decoupled and have different group velocities,  $u_1$  and  $u_2$ . Each mode, described by the boson field  $\varphi_i$  and its dual  $\vartheta_i$ , is a superposition of the spin up and down fields  $\phi_\sigma$  and  $\theta_\sigma$ ,

$$\begin{pmatrix} \varphi_1 \\ \varphi_2 \end{pmatrix} = (\bar{Z}^T)^{-1} \begin{pmatrix} -\phi_\uparrow \\ \phi_\downarrow \end{pmatrix}, \quad \begin{pmatrix} \vartheta_1 \\ \vartheta_2 \end{pmatrix} = \bar{Z} \begin{pmatrix} -\theta_\uparrow \\ \theta_\downarrow \end{pmatrix}. \quad (9)$$

The superscript T means matrix transpose, and the so-called dressed charge matrix is given by

$$\bar{Z} = \begin{bmatrix} Z_{cc} - Z_{sc} & Z_{sc} \\ Z_{ss} - Z_{cs} & -Z_{ss} \end{bmatrix}. \quad (10)$$

Eq. (9) clearly shows that in general each normal mode  $\varphi_i$  is a mixture of the spin field  $\phi_s$  and the charge field  $\phi_c$ . Therefore, elementary excitations of the FFLO state are

fractional states carrying both charge and spin, i.e., the superposition of spinons and holons [31]. The degree of spin-charge mixing is determined by the dressed charge matrix  $\bar{Z}$ , or equivalently matrix  $\bar{Y} \equiv [\bar{Z}^T]^{-1}$  [30, 31, 32, 33]. As shown in Ref. [31], spin-charge separation occurs only if the charge matrix

$$\hat{g} \equiv \bar{Z}^{-1}\bar{Y}$$

possesses a  $Z_2$  symmetry,  $g_{11} = g_{22}$ ,  $g_{12} = g_{21}$ , i.e.,  $\hat{g}$  is invariant under the exchange  $1 \leftrightarrow 2$ . All the parameters in the effective bosonized Hamiltonian  $H_{\text{FFLO}}$ , such as  $\{\bar{Z}_{ij}, u_i\}$ , can be computed from the parameters of the microscopic Hamiltonian  $H_{GY}$  or  $H_U$ . Eq. (8)-(10) are the main results of this section, they form the basis for all subsequent discussions on correlation functions and quasi-1D phases.

## B. The method

Below we outline the main steps leading to the effective field theory Eq. (8) and the algorithm to compute parameters  $\{\bar{Z}_{ij}, u_i\}$ . The procedure takes a detour to make use of several well established, nontrivial results for the 1D Hubbard model.

(I) We start from the attractive Hubbard model  $H_U$ . Its continuum limit, summarized in Eq. (3), yields the Gaudin-Yang model  $H_{GY}$ . Therefore, in this limit, the effective field theory of the two models are the same. Indeed, there is a one to one correspondence between the Bethe ansatz integral equation for the Hubbard model [23] and the Gaudin integral equation for Gaudin-Yang model [34]. In principal, all analysis can be performed on the Gaudin-Yang model directly without resorting to its lattice regularization to arrive at the same conclusion. In practice, however, the latter route is less economical since the Bethe ansatz solution of the continuum model, especially its dressed charge formalism, is less developed.

(II) We map the attractive Hubbard model  $H_U$  for given  $(U/t, n, p)$  to a repulsive Hubbard model  $H'_U$  with onsite repulsion  $U$ , density  $n' = 1 - np$ , and imbalance  $p' = (1-n)/(1-np)$  by the well-known staggered particle-hole transformation [23, 35, 36, 37],

$$c_{i,\uparrow} \rightarrow (-1)^i c_{i,\uparrow}^\dagger, \quad c_{i,\downarrow} \rightarrow c_{i,\downarrow}. \quad (11)$$

The motivation behind this is two-fold. First, it is technically more convenient to solve  $H'_U$  via Bethe ansatz [35]. Second, as shown by Penc and Sólyom [38] based on the work of Frahm and Korepin [30], the repulsive Hubbard model at general (non-half) filling and magnetic field is equivalent to a two-component Tomonaga-Luttinger (TL) liquid. We shall exploit this result to construct the field theory for  $H_U$  (and  $H_{GY}$ ) from the Bethe ansatz solution of  $H'_U$ .

(III) For given  $(U/t, n', p')$ , we numerically solve the coupled Bethe ansatz integral equations for  $H'_U$ . We first determine the density distribution functions  $\rho(k)$

and  $\sigma(\lambda)$ , defined within the Fermi interval  $k \in (-Q, Q)$  and spin rapidity range  $\lambda \in (-A, A)$  respectively. This requires solving

$$\begin{aligned} \rho(k) &= \frac{1}{2\pi} + \cos k \int_{-A}^A d\lambda a_1(\sin k - \lambda)\sigma(\lambda), \\ \sigma(\lambda) &= \int_{-Q}^Q dk \rho(k) a_1(\sin k - \lambda) \\ &\quad - \int_{-A}^A d\lambda' \sigma(\lambda') a_2(\lambda - \lambda'), \end{aligned}$$

where  $a_n(x) = nU/(4\pi t)/[(U/4t)^2 + x^2]$ , together with the number constraint equations,

$$\begin{aligned} \int_{-Q}^Q dk \rho(k) &= n', \\ \int_{-A}^A d\lambda \sigma(\lambda) &= n'_\downarrow = \frac{n'}{2}(1 - p'). \end{aligned}$$

This is done by an iteration procedure which also fixes  $Q$  and  $A$  self-consistently. Each integral equation is converted to an algebraic equation using Gaussian-Legendre quadrature. The code was checked to yield exactly the same result as those in Ref. [30, 38].

Once  $Q$  and  $A$  are found, it is then straightforward to find other quantities: the dressed energies  $[\epsilon_c(k), \epsilon_s(\lambda)]$ , their derivatives,  $[\epsilon'_c(k), \epsilon'_s(\lambda)]$ , and the dressed charges,  $[\xi_{cc}(k), \xi_{cs}(\lambda), \xi_{sc}(k), \xi_{ss}(\lambda)]$ , by solving corresponding integral equations. These lengthy equations are well documented and will not be repeated here [23, 30, 38]. The dressed charge matrix elements are given by

$$\begin{aligned} Z_{cc} &= \xi_{cc}(Q), \quad Z_{cs} = \xi_{cs}(A), \\ Z_{sc} &= \xi_{sc}(Q), \quad Z_{ss} = \xi_{ss}(A). \end{aligned}$$

The normal mode group velocities are,

$$u_1 = \frac{\epsilon'_c(Q)}{2\pi\rho(Q)}, \quad u_2 = \frac{\epsilon'_s(A)}{2\pi\sigma(A)}.$$

Note that the subscripts  $c$  and  $s$  here and in the Bethe ansatz literature have to be distinguished from the charge and spin index in Abelian bosonization such as in Eq. (7). This fact has been emphasized for example by Voit et al [39]. To avoid confusion, we adopt index  $i = 1, 2$  to label the two normal modes instead of  $c$  and  $s$ .

(IV) We map  $H'_U$  to a two-component Tomonaga-Luttinger Hamiltonian,  $H'_{TL}$ , following Penc and Sólyom [38]. It becomes transparent in bosonized form

$$\begin{aligned} H'_{TL} &= \int \frac{dx}{2\pi} [(v_{f,\uparrow} + \tilde{g}_{4,\uparrow} - \tilde{g}_{2,\uparrow})(\nabla\theta_\uparrow)^2 \\ &\quad + (v_{f,\uparrow} + \tilde{g}_{4,\uparrow} + \tilde{g}_{2,\uparrow})(\nabla\phi_\uparrow)^2 \\ &\quad + (v_{f,\downarrow} + \tilde{g}_{4,\downarrow} - \tilde{g}_{2,\downarrow})(\nabla\theta_\downarrow)^2 \\ &\quad + (v_{f,\downarrow} + \tilde{g}_{4,\downarrow} + \tilde{g}_{2,\downarrow})(\nabla\phi_\downarrow)^2 \\ &\quad + 2(\tilde{g}_{4,\perp} - \tilde{g}_{2,\perp})\nabla\theta_\uparrow\nabla\theta_\downarrow + 2(\tilde{g}_{4,\perp} + \tilde{g}_{2,\perp})\nabla\phi_\uparrow\nabla\phi_\downarrow]. \end{aligned}$$

The Luttinger parameters in the g-ology notation,  $\tilde{g}$ , are given in terms of  $\{u_i, Z_{ij}\}$  by Eq. (6.12) to (6.17) in Ref. 38. For example,

$$\begin{aligned} v_{f,\uparrow} + \tilde{g}_{4,\uparrow} - \tilde{g}_{2,\uparrow} &= u_1(z_{cc} - Z_{sc})^2 + u_2(Z_{cs} - Z_{ss})^2, \\ v_{f,\uparrow} + \tilde{g}_{4,\uparrow} + \tilde{g}_{2,\uparrow} &= \frac{u_1 Z_{ss}^2 + u_2 Z_{sc}^2}{(Z_{cc} Z_{ss} - Z_{cs} Z_{sc})^2}. \end{aligned}$$

The low energy effective theory  $H'_{TL}$  yields the same finite size spectrum and correlation functions as the original microscopic model  $H'_U$ . It is instructive to compare this nonperturbative result with that obtained by weak coupling bosonization,  $H_B$  in Eq., (7).

(V) Finally we particle-hole transform  $H'_{TL}$  back to obtain the effective Hamiltonian  $H_{TL}$  for  $H_U$ . In bosonized form,  $H_{TL}$  is obtained from  $H'_{TL}$  by replacement  $\phi_\uparrow \rightarrow -\phi_\uparrow$  and  $\theta_\uparrow \rightarrow -\theta_\uparrow$ . Since  $H_{TL}$  is quadratic, we diagonalize it by a canonical transformation using matrix  $\bar{Z}$  [31, 32]. The end result is Eq. (8).

## V. SINGLE PARTICLE AND PAIR CORRELATION FUNCTIONS

The bosonized effective Hamiltonian Eq. (8) makes it straightforward to compute the correlation function of any operator of the form

$$O(x) = e^{i[\hat{a}^T \hat{\phi}(x) + \hat{b}^T \hat{\theta}(x)]}$$

where  $\hat{a}$  and  $\hat{b}$  are arbitrary two-component vectors, and  $\hat{\phi}^T = (\phi_\uparrow, \phi_\downarrow)$ ,  $\hat{\theta}^T = (\theta_\uparrow, \theta_\downarrow)$ . Using the relation Eq. (9), we find that the correlation function  $\langle O(x)O^\dagger(0) \rangle$  has the asymptotic behavior of  $x^{-2\delta}$  at zero temperature as  $x \rightarrow \infty$ . The scaling dimension of  $O$  is given by

$$\delta = \frac{1}{4}[\hat{a}^T \hat{g}^{-1} \hat{a} + \hat{b}^T \hat{g} \hat{b}].$$

The charge matrix is defined by  $\hat{g} = \bar{Z}^{-1} \bar{Y}$ .

We apply this result to compute the single particle propagator and the singlet pair susceptibility

$$\begin{aligned} G_\sigma(x, \tau) &= -\langle T_\tau \psi_{R,\sigma}(x, \tau) \psi_{R,\sigma}^\dagger(0, 0) \rangle, \\ \chi(x, \tau) &= -\langle T_\tau \Delta(x, \tau) \Delta^\dagger(0, 0) \rangle. \end{aligned} \quad (12)$$

We shall focus on  $G_\uparrow$  for the majority spin ( $\uparrow$ ), since  $G_\downarrow$  only has subdominant power law divergence (its scaling dimension is larger than that of  $G_\uparrow$ , i.e.,  $\delta_\downarrow > \delta_\uparrow$ ). For example, from the bosonized representation of fermion field operator  $\psi_{R,\sigma}$ , Eq. (6), we find  $a = (-1, 0)^T$  and  $b = (1, 0)^T$  for  $G_\uparrow$ . It follows that for  $x \rightarrow \infty$  at zero temperature,

$$G_\uparrow(x) \sim \frac{e^{ik_{f\uparrow}x}}{x^{2\delta_\uparrow}}, \quad \delta_\uparrow = \beta_1 + \beta_2, \quad (13)$$

$$\chi(x) \sim \frac{e^{iq_*x}}{x^{2\delta_\Delta}}, \quad \delta_\Delta = \gamma_1 + \gamma_2. \quad (14)$$

The scaling dimensions of the single particle field operator  $\psi_\uparrow$  and pair operator  $\Delta$  are directly related to the dress charge matrix elements that describe the effect of spin-charge mixing,

$$\begin{aligned} \beta_1 &= \frac{1}{4}[(\bar{Z}_{11})^2 + (\bar{Y}_{11})^2], & \beta_2 &= \frac{1}{4}[(\bar{Z}_{21})^2 + (\bar{Y}_{21})^2]; \\ \gamma_1 &= \frac{1}{4}[Z_{cc}^2 + \frac{Z_{cs}^2}{(\det \bar{Z})^2}], & \gamma_2 &= \frac{1}{4}[Z_{cs}^2 + \frac{Z_{cc}^2}{(\det \bar{Z})^2}]. \end{aligned} \quad (15)$$

Here  $\bar{Z}_{11}$  denotes the (1,1) element of the matrix  $\bar{Z}$ . We also define the corresponding anomalous dimensions  $\eta_\uparrow = 2 - 2\delta_\uparrow$ , and  $\eta_\Delta = 2 - 2\delta_\Delta$ .

Eq. (14) is the hallmark of 1D FFLO phase: the  $s$ -wave pair correlation function oscillates in space at the FFLO wave vector  $q_* = k_{f,\uparrow} - k_{f,\downarrow}$  on top of the algebraic decay. Although it looks similar to Yang's conclusion based the spin-charge separated model  $H_Y$ , the present result fully takes into account the effect of spin-charge mixing and remains valid for all values of  $0 < p < 1$ . Our results can also shed more light on the nature of the magnetic field driven BCS-FFLO transition in 1D. Under a particle-hole transformation, it is equivalent to the Mott transition of repulsive Fermi gas in magnetic field (driven by varying chemical potential). As shown recently by Frahm and Vekua [32], due to the intrinsic spin-charge coupling, it is *not* in the same universality class as the single mode commensurate-incommensurate transition.

At finite temperature  $T$ ,  $G_\uparrow(x, \tau)$  and  $\chi(x, \tau)$  still factorize due to the decoupling of two normal modes. After some algebra, we obtain the Fourier component  $G_0 = G_\uparrow(k = k_{f,\uparrow}, \omega = 0)$  (up to a phase factor),

$$G_0 = (2\pi^3 \alpha T^2)^{-1} I_1 \left( \frac{u_1}{u_2} \right) \prod_{i=1,2} \left( \frac{\pi T \alpha}{u_i} \right)^{2\beta_i} \sqrt{u_i}. \quad (16)$$

Similarly,  $\chi_0 = \chi(k = q_*, \omega = 0)$  is found to be

$$\chi_0 = (2\pi^2 \alpha T)^{-2} I_2 \left( \frac{u_1}{u_2} \right) \prod_{i=1,2} \left( \frac{\pi T \alpha}{u_i} \right)^{2\gamma_i} \sqrt{u_i}. \quad (17)$$

Here, the dimensionless function  $I_{1/2}$  are defined as

$$\begin{aligned} I_1(y) &= \int_{-\infty}^{\infty} dx \int_0^\pi dt \sin t \prod_i [\sinh^2(xy^{i-\frac{3}{2}}) + \sin^2(t)]^{-\beta_i}, \\ I_2(y) &= \int_{-\infty}^{\infty} dx \int_0^\pi dt \prod_i [\sinh^2(xy^{i-\frac{3}{2}}) + \sin^2(t)]^{-\gamma_i}. \end{aligned}$$

These results will become useful in the RPA calculation for the quasi-1D systems. Note that the ratio  $u_1/u_2$  is not a rapidly changing function of  $\gamma$ . Fig. 1 shows its value for  $p = 0.2$ .

## VI. PHASE DIAGRAM OF THE QUASI-1D SYSTEM AT $T = 0$ .

We now apply the effective theory for single tube to study the quasi-1D system realized in experiments: a

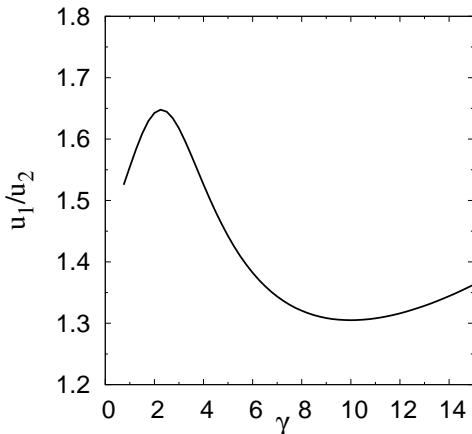


FIG. 1: The ratio  $u_1/u_2$  as function of  $\gamma$  for  $p = 0.2$ .

square lattice array of such tubes coupled by transverse hopping  $t_\perp$ . We are interested in the fate of the 1D FFLO phase as the  $t_\perp$  is turned on.

In the limit of small  $t_\perp$ , we can treat  $H_\perp$  and  $H_J$  as perturbations to the individual 1D Hamiltonian  $H_{\text{FFLO}}$ . In the language of renormalization group (RG), both  $H_\perp$  and  $H_J$  are relevant perturbations: the scaling dimensions of the single particle and pair tunneling are both smaller than 2. The first-order RG equations for the effective inter-tube couplings  $t_\perp(\kappa)$  and  $J(\kappa)$  at momentum scale  $\kappa$  (with  $\kappa \rightarrow 0$ ) read:

$$\begin{aligned} \kappa dt_\perp(\kappa)/d\kappa &= (2\delta_\uparrow - 2)t_\perp(\kappa), \\ \kappa dJ(\kappa)/d\kappa &= (2\delta_\Delta - 2)J(\kappa), \end{aligned} \quad (18)$$

where the equation of  $t_\perp$  is for the spin  $\uparrow$  tunneling (as we have emphasized before, it is more relevant than the spin  $\downarrow$ ). In other words, the fate of the 1D FFLO phase is controlled by the relative magnitude  $\delta_\uparrow$  and  $\delta_\Delta$  [17]. For  $\delta_\Delta < \delta_\uparrow$ , pair tunneling is most relevant and the system flows into a quasi-1D FFLO state. In this state, strong effective Josephson coupling locks the phases of all tubes to establish the overall phase coherence to produce a genuine superfluid state. For  $\delta_\Delta > \delta_\uparrow$ , however, single particle tunneling is most relevant and the system flows into a partially polarized Fermi liquid (FL) state with well defined quasiparticles. In the latter case, the actual ground state of the quasi-1D system at zero temperature depends on the residue interactions between quasiparticles, the details of which are not captured by the leading order RG analysis presented here [17]. Such limited predictive power is inherent to all leading order RG analysis on coupled Luttinger liquids. Therefore, the Fermi liquid state predicted here should be understood as a region in the phase diagram where the superfluid transition temperature is significantly suppressed by the weakening of effective intertube Josephson coupling. It is important to bear in mind that other instabilities may take over at lower temperatures leading to a ground state with broken symmetry.

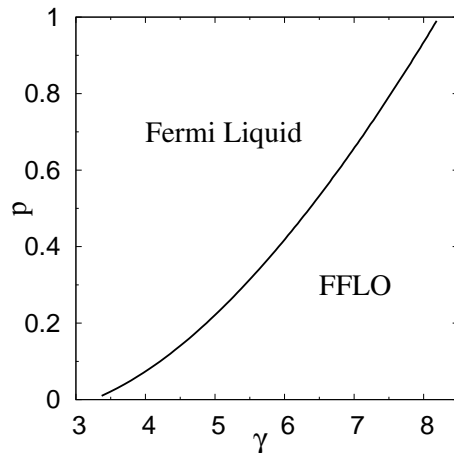


FIG. 2: Zero temperature phase diagram of a quasi-1D attractive Fermi gas in the limit of weak inter-tube tunneling.  $\gamma$  is the interaction strength of the Gaudin-Yang model and  $p$  is the population imbalance.

The  $T = 0$  phase diagram of the quasi-1D gas system based on leading order RG is shown in Fig. 2. It is obtained by going through the steps outlined in Sec.IV B and taking the continuum limit,  $a \rightarrow 0$ , for fixed particle numbers and system length  $L$  [see Eq. (3)]. As the intertube tunneling is turned on, the 1D FFLO phase (originally occupying the whole region  $0 < p < 1$  for all  $\gamma$ ) splits into two distinct phases, an FFLO superfluid and a polarized Fermi liquid (FL). Intuitively, stronger attractive interaction (larger  $\gamma$ ) favors the FFLO phase. From Fig. 2, one can read off the critical interaction strength required to realize the quasi-1D FFLO state for given  $p$ . For fixed interaction  $\gamma$ , increasing imbalance would drive the system out of FFLO into a Fermi liquid phase. A crucial feature of the phase diagram is that the FFLO phase survives in a smaller region in quasi-1D than true 1D (single tube). This shrinking trend observed at  $t_\perp \rightarrow 0$  is expected to continue as  $t_\perp$  increases, since we know that FFLO state in 3D only occupies a tiny part of the phase diagram [8]. Fig. 3 shows  $T = 0$  phase diagram of the quasi-1D attractive Hubbard model in the limit of  $t_\perp \rightarrow 0$ . We observe a similar splitting of the 1D FFLO phase. Ref. 37 also discussed the phases of weakly coupled Hubbard chains in the presence of finite spin polarization, close in spirit with ours. While our main focus here is the continuous gas systems (without lattice in the  $x$  direction), our result of quasi-1D Hubbard model (Figure 3) agrees with Ref. 37.

## VII. THE TRANSITION TEMPERATURE OF QUASI-1D FFLO STATE

In this section, we use the random phase approximation (RPA) [16, 40, 41] to compute the FFLO superfluid transition temperature  $T_c$  for the quasi-1D system with

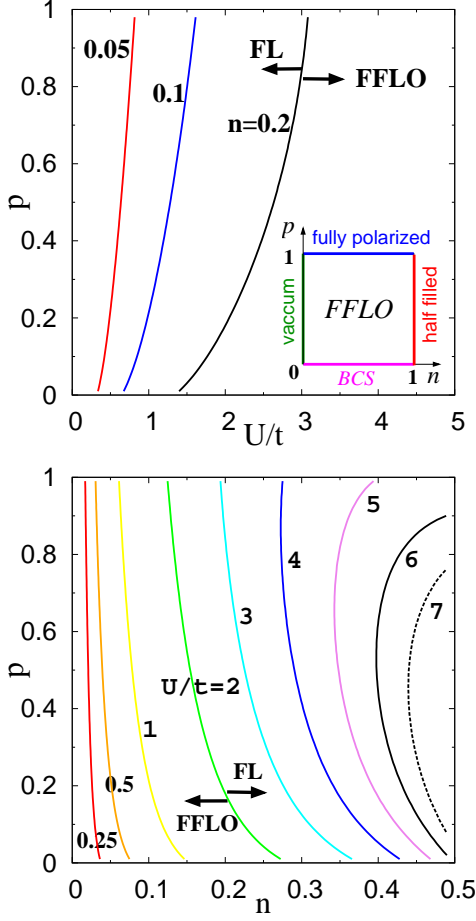


FIG. 3: (Color online) Zero temperature phase diagram of the quasi-1D attractive Hubbard model,  $H_U + H_\perp + H_J$ , in the limit of small  $t_\perp$ .  $p$  is the population imbalance. Each line for fixed density  $n$  (top panel) or interaction strength  $U/t$  (bottom panel) is the phase boundary separating the FFLO and Fermi liquid (FL) phase (indicated by arrows). Inset: phase diagram of the 1D attractive Hubbard model (single tube).

a small but finite  $t_\perp$ , going beyond the perturbative RG analysis in the previous section. RPA has been successfully applied to study coupled Luttinger liquids ( $p = 0$ ) [41]. Here we generalize it to the case of  $p > 0$  with spin-charge mixing. Within RPA, the 3D single particle propagator

$$\mathcal{G}_\uparrow^{-1}(k, k_\perp = 0, \omega_n) = G_\uparrow^{-1}(k, \omega_n) - z_\perp t_\perp, \quad (19)$$

and the 3D pair susceptibility

$$\mathcal{X}^{-1}(q_*, k_\perp = 0, \omega = 0) = \chi_0^{-1} - z_\perp J, \quad (20)$$

where  $k_\perp$  is the transverse momentum and  $z_\perp = 4$  is the transverse coordination number of every single atomic gas tube in a square lattice array. The 1D propagator  $G_\downarrow$  and susceptibility  $\chi_0$  have been computed in Section V and are given by Eq. (16) and (17), respectively.

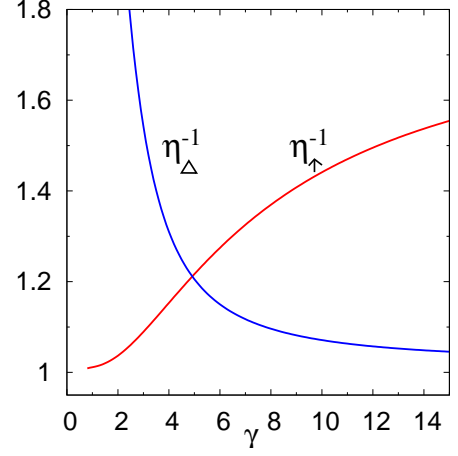


FIG. 4: RPA predictions for the  $t_\perp$  dependence of the single particle crossover (Luttinger liquid to Fermi liquid) temperature,  $T_{\text{FL}} \sim t_\perp^{1/\eta_\uparrow}$ , and the FFLO transition temperature,  $T_c \sim t_\perp^{2/\eta_\Delta}$ , as functions of  $\gamma$  for  $p = 0.2$ .

RPA predicts two temperature scales that characterize the 1D-to-3D crossover as the temperature is lowered.  $\mathcal{G}_\uparrow(k_{f\uparrow}, 0, \omega_{n=1})$  starts to develop a pole at the single particle crossover temperature  $T_{\text{FL}}$ . From Eq. (19), we find

$$T_{\text{FL}} \sim W \left[ \frac{t_\perp z_\perp}{W} \text{I}_1\left(\frac{u_1}{u_2}\right) \right]^{1/\eta_\uparrow} \prod_i \left( \frac{u_i}{\bar{v}_f} \right)^{(1/2 - 2\beta_i)/\eta_\uparrow}. \quad (21)$$

Similarly, the divergence of the 3D pair susceptibility  $\mathcal{X}(q_*, 0, 0)$  defines the two particle crossover temperature  $T_c$ ,

$$T_c \sim W \left[ \frac{J z_\perp}{\bar{v}_f} \text{I}_2\left(\frac{u_1}{u_2}\right) \right]^{1/\eta_\Delta} \prod_i \left( \frac{u_i}{\bar{v}_f} \right)^{(1/2 - 2\gamma_i)/\eta_\Delta}. \quad (22)$$

Here the ultraviolet cutoff  $W = \bar{v}_f/\alpha$  is roughly the band width (or Fermi energy). Above  $\max(T_{\text{FL}}, T_c)$ , thermal fluctuation destroys coherence between the tubes, the system behaves as uncoupled two-component Luttinger liquids with fractional excitations, each described by  $H_{\text{FFLO}}$ . As the temperature is lowered, if  $T_{\text{FL}} > T_c$ , these fractional excitations first confine into sharply defined quasiparticles at temperature scale  $T_{\text{FL}}$ , and the system crosses over to a partially polarized Fermi liquid (the Fermi liquid may develop other instabilities at lower temperature depending on the details of the residue interactions between the quasiparticles). On the other hand, if  $T_c > T_{\text{FL}}$ , the system first undergoes a phase transition into an FFLO phase with long range order. In this case,  $T_c$  can be identified as the superfluid transition temperature. In the limit of vanishing  $p$ , the transition into the FFLO superfluid can be viewed as the condensation of soliton liquid into crystal, i.e. static domain walls [17].

Whether the single or two particle crossover occurs first depends on the interaction strength. At low densities, we find from Eq. (21) and (22) that  $T_{\text{FL}} > T_c$  at small

$\gamma$  (weak interaction) while  $T_c > T_{\text{FL}}$  for large  $\gamma$  (strong interaction). Thus, the schematic plot of  $T_{\text{FL}}$  and  $T_c$  as functions of  $\gamma$  looks similar to Fig. 1 of Ref. [41] for coupled Luttinger liquids. At some critical value of  $\gamma$ ,  $T_{\text{FL}}$  and  $T_c$  are comparable to each other. This marks the phase boundary between the Fermi liquid and the FFLO phase. All these results are in qualitative agreement with those obtained in the previous section from RG analysis.

Eq. (22) shows that  $T_c$  scales with  $J$  as a power law, with the exponent given by the inverse of anomalous dimension  $\eta_\Delta$ ,

$$T_c \propto J^{1/\eta_\Delta}.$$

The exponents  $\eta_\Delta^{-1}$  and  $\eta_\uparrow^{-1}$  are plotted in Fig. 4 for  $p = 0.2$ . We observe that at weak interaction  $T_{\text{FL}} \propto t_\perp$ , while at strong interaction  $T_c \propto J \propto t_\perp^2$ . The growth of  $T_c$  with

inter-tube coupling will eventually stop when  $t_\perp$  becomes so large that it can no longer be treated as a perturbation. Then the system becomes more 3D-like, and  $T_c$  starts to drop as  $t_\perp$  is further increased [14]. Our results support the argument of Ref. [14] that the optimal value of  $T_c$  is realized for small but finite  $t_\perp$ .

### Acknowledgments

We thank M. A. Cazalilla, A. Ho, D. Huse, A. Paramekanti, and especially R. Hulet for illuminating discussions. This work is supported under ARO Award No. W911NF-07-1-0464 with funds from the DARPA OLE Program and ARO Award No. W911NF-07-1-0293.

- 
- [1] G. B. Partridge, W. Li, R. I. Kamar, Y.-A. Liao, and R. G. Hulet, *Science* 311, 503 (2006).
  - [2] M. W. Zwierlein, A. Schirotzek, C. H. Schunck, and W. Ketterle, *Science* 311, 492 (2006).
  - [3] M. W. Zwierlein, C. H. Schunck, A. Schirotzek, and W. Ketterle, *Nature* 442, 54 (2006).
  - [4] Y. Shin, M. W. Zwierlein, C. H. Schunck, A. Schirotzek, and W. Ketterle, *Phys. Rev. Lett.* 97, 030401 (2006).
  - [5] G. B. Partridge, W. Li, Y. A. Liao, R. G. Hulet, M. Haque, and H. T. C. Stoof, *Phys. Rev. Lett.* 97, 190407 (2006).
  - [6] C. H. Schunck, Y. Shin, A. Schirotzek, M. W. Zwierlein, and W. Ketterle, *Science* 316, 867 (2007).
  - [7] R. Casalbuoni and G. Nardulli, *Rev. Mod. Phys.* 76, 263 (2004).
  - [8] D. E. Sheehy and L. Radzihovsky, *Ann. Phys.* 322, 1790 (2007), and references therein.
  - [9] G. Orso, *Phys. Rev. Lett.* 98, 070402 (2007).
  - [10] H. Hu, X.-J. Liu, and P. D. Drummond, *Phys. Rev. Lett.* 98, 070403 (2007); *Phys. Rev. A* 76, 043605 (2007).
  - [11] X. W. Guan et al, *Phys. Rev. B* 76, 085120 (2007).
  - [12] A. E. Feiguin and F. Heidrich-Meisner, *Phys. Rev. B* 76, 220508 (R) (2007); M. Tezuka and M. Ueda, *Phys. Rev. Lett.* 100, 110403 (2008).
  - [13] M. Rizzi, M. Polini, M. A. Cazalilla, M. R. Bakhtiari, M.P. Tosi, R. Fazio, *Phys. Rev. B* 77, 245105 (2008).
  - [14] M. M. Parish, S. K. Baur, E. J. Mueller, and D. A. Huse, *Phys. Rev. Lett.* 99, 250403 (2007).
  - [15] H. Moritz, T. Stöferle, K. Günter, M. Köhl, and T. Esslinger, *Phys. Rev. Lett.* 94, 210401 (2005).
  - [16] H. J. Schulz and C. Bourbonnais, *Phys. Rev. B* 27, 5856 (1983); E. W. Carlson, D. Orgad, S. A. Kivelson, and V. J. Emery, *Phys. Rev. B* 62, 3422 (2000).
  - [17] K. Yang, *Phys. Rev. B* 63, 140511(R) (2001).
  - [18] C. N. Yang, *Phys. Rev. Lett.* 19, 1312 (1967).
  - [19] M. Gaudin, *Phys. Lett. A* 24, 55 (1967).
  - [20] M. Olshanii, *Phys. Rev. Lett.* 81, 938 (1998).
  - [21] T. Bergeman, M. G. Moore, and M. Olshanii, *Phys. Rev. Lett.* 91, 163201 (2003).
  - [22] M. Casula, D. M. Ceperley, E. J. Mueller, *Phys. Rev. A* 78, 033607 (2008).
  - [23] F. H. L. Essler, H. Frahm, F. Göhmann, A. Klümper, and V. E. Korepin, *The one dimensional Hubbard model*, Cambridge University Press, Cambridge (2005).
  - [24] R. Hulet, private communications.
  - [25] T. Giamarchi, *Quantum physics in one dimension*, Oxford University Press, Oxford (2004).
  - [26] A. O. Gogolin, A. A. Nersesyan, A. M. Tsvelik, *Bosonization and strongly correlated systems*, Cambridge University Press, Cambridge (1998).
  - [27] F. D. M. Haldane, *J. Phys. A* 15, 507 (1982).
  - [28] G. I. Japaridze and A. A. Nersesyan, *JETP Lett.* 27, 334 (1978).
  - [29] H. Burkhardt and D. Rainer, *Ann. Phys.* 3, 181 (1994).
  - [30] H. Frahm and V. E. Korepin, *Phys. Rev. B* 42, 10 553 (1990); *Phys. Rev. B* 43, 5653 (1991).
  - [31] K.-V. Pham, M. Gabay, and P. Lederer, *Phys. Rev. B* 61, 16397 (2000).
  - [32] H. Frahm and T. Vekua, *J. Stat. Mech.* P01007, (2008).
  - [33] T. Hikihara, A. Furusaki, and K. A. Matveev, *Phys. Rev. B* 72, 035301 (2005).
  - [34] M. Takahashi, *Thermodynamics of one-dimensional solvable models*, Cambridge University Press, Cambridge (1999).
  - [35] T. B. Bahder and F. Woynarovich, *Phys. Rev. B* 33, 2114 (1986).
  - [36] V. J. Emery, *Phys. Rev. B* 14, 2989 (1976); A. Moreo and D. J. Scalapino, *Phys. Rev. Lett.* 98, 216402 (2007);
  - [37] A. Lüscher, R. M. Noack, and A. M. Läuchli, *Phys. Rev. A* 78, 013637 (2008).
  - [38] K. Penc and J. Sólyom, *Phys. Rev. B* 47, 6273 (1993).
  - [39] J. Voit, Y. Wang, and M. Grioni, *Phys. Rev. B* 61, 7930 (2000).
  - [40] X.-G. Wen, *Phys. Rev. B* 42, 6623 (1990).
  - [41] D. Boies, C. Bourbonnais, and A.-M. S. Tremblay, *Phys. Rev. Lett.* 74, 968 (1995).